Pure & Appl. Chem., Vol. 59, No. 1, pp. 79–90, 1987.
Printed in Great Britain.

Kinetics of phase separation in fluid mixtures by relaxation methods: Pressure-jump experiments and selected results

Gerhard M. Schneider, Michael Dittmann, Ute Metz, and Jürgen Wenzel

Physical Chemistry Laboratory, Department of Chemistry, University of Bochum, D-4630 Bochum, Federal Republic of Germany

Abstract - The investigation of a physico-chemical system in a non-equilibrium state as a function of time needs carefully designed experimental methods. The present paper refers to an adaption of relaxation techniques to the investigation of the kinetics of phase separation in fluid mixtures by the use of a fast pressure jump technique. Methods and experimental set-ups are described that allowed us to investigate the transmitted and scattered light intensities as closely as possible to the first formation of droplets after a pressure-jump induced phase separation. By evaluation of transient Mie scattering spectra from phase separation processes the existence of a kinetic barrier inside the coexistence region was established and its location inside the phase diagram could be determined. In addition an apparatus for the phenomenological investigation of late stages of phase separation (like aggregation and segregation) with the use of micro and macro photography is described. Recent developments will be reported on applying pressure jump techniques to gas-liquid mixtures and improving them to the performance of differential pressure jumps with nearly arbitrary initial and final pressures. Applications on isopycnic systems are discussed in order to simulate the absence of gravitational forces.

INTRODUCTION

Section 7 of the 9th IUPAC Conference on Chemical Thermodynamics, 14 - 18 July 1986, Lisbon, Portugal, was concerned with 'Modern Techniques' (Chairmen: J.C.G. Calado, G.M. Schneider), a promising and rapidly developing and expanding field of science because of the enormous progress that has been obtained in measuring techniques and computerization during the last two decades. Invited lectures were given by J. Thoen, Leuven, Belgium, on high-resolution calorimetry on liquid crystals (ref. 1), Y. Takahashi, Tokyo, Japan, on laser-flash calorimetry (ref. 14) as well as A.L. Ruoff, Cornell University, Ithaca, N.Y., USA (ref. 17), and J.A. Schouten, Amsterdam, Netherlands (ref. 18), on diamond anvil experiments on solids in the megabar range and on fluid rare gas mixtures up to 100 kbar respectively. The accent of the contributed papers was on calorimetry (refs 2 - 7, 15, 16) where modern high-pressure applications were also discussed (refs. 2, 3, 5, 7); pVT (refs 8 - 10) and ultrasonic techniques (refs 11 - 13) as well as phase equilibrium investigations (refs 19, 20) were also presented.

In the following investigations on the kinetics of phase separation in fluid mixtures by relaxation techniques that have been performed at the University of Bochum will be presented and discussed in detail (ref. 21). At the Conference most of the results were illustrated by a silent 16 mm film; in the present paper documentation has, however, to be made by diagrams and photographs.

Whereas the equilibrium properties of heterogeneous systems have been widely investigated and play an important role in science and technology (e.g. for some separation techniques), little is known about the rate of formation and growth of a new phase that is formed when penetrating the two-phase region. The thermodynamic conditions for phase separation in fluid binary mixtures can be deduced from Fig. 1. In Fig. 1c a schematic $T(x_1)$ phase diagram for p = const with the exhibition of an upper critical solution temperature (UCST) is given whereas in Fig. 1d a schematic $p(x_1)$ phase diagram for T = const with the exhibition of a lower critical solution pressure (LCSP) is represented (x_1 = mole fraction of component 1). The type given in Fig. 1 corresponds to a binary

system that exhibits an UCST which rises with increasing pressure such as found e.g. for cyclohexane + methanol; a schematic three-dimensional representation of the pTx immiscibility surface is given in Fig. 13. For a systematic discussion of liquid-liquid phase behaviour as a function of pressure see ref. 22.

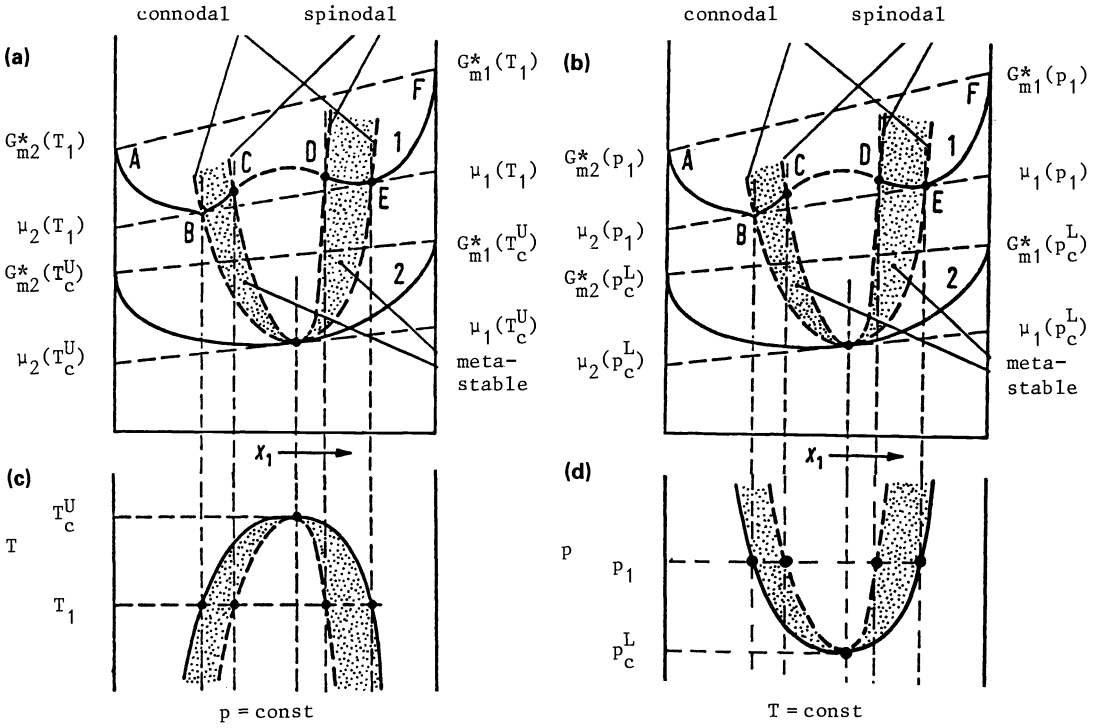

Fig. 1. Thermodynamic conditions for phase separation in binary fluid mixtures (see text; the metastable region is dotted)
Fig. 1a and 1c. $G_m(x_1)$ isotherms and $T(x_1)$ phase diagram at p = const for a binary system with an upper critical solution temperature (UCST)
Fig. 1b and 1d. $G_m(x_1)$ isobars and $p(x_1)$ phase diagram at T = const for a binary system with a lower critical solution pressure (LCSP)

In the upper part of Fig. 1 the corresponding $G_m(x_1)$ curves (where G_m = molar Gibbs energy) for two different temperatures T_1 and T_c^U (= UCST) at a constant pressure p (Fig. 1a) and for two different pressures p_1 and p_c^L (= LCSP) at a constant temperature T (Fig. 1b) are given. The coexistence curves (= connodals) in Fig. 1c and 1d are obtained from the common tangents at B and E of the $G_m(x_1)$ curves for T_1 = const or p_1 = const respectively. The spinodals are derived from the inflection points C and D of these curves where $(\partial^2 G_m/\partial x_1^2)_{p,T} = 0$ (or $D_{12} = 0$ with D_{12} = binary diffusion coefficient). At a critical point CP the points B, C, D and E coincide and the additional condition $(\partial^3 G_m/\partial x_1^3)_{p,T} = 0$ holds. Between C and D the curvature of the isothermal-isobaric $G_m(x_1)$ curves is negative giving rise to absolute instability of a one-phase state whereas between B and C as well as D and E two phases are stable but one phase can exist in a metastable state. Between A and B as well as E and F homogeneous states are stable. For a detailed discussion of the thermodynamic background (especially with respect to material and diffusional instability) see e.g. ref. 38.

Fig. 1c is again schematically represented in Fig. 2; in principle it holds for all kinds of fluid-fluid phase equilibria (e.g. liquid-liquid, gas-liquid). From the existence of a spinodal inside the connodal curve some important consequences can be deduced for the kinetics of phase separation in fluid mixtures. When entering the metastable range relatively far away from CP (e.g. by a negative temperature jump) phase separation is initiated by nucleation the growth of the nuclei being slow for slight and fast for great supersaturations respectively. When approaching CP of a gas-liquid system homogeneous concurs more and more with heterogeneous phase formation. At CP the unstable region is entered and spontaneous phase separation takes place (= spinodal decomposition). This paper is concerned with some experimental techniques that have been developed at Bochum in order to study off-critical and near-critical effects whereas spinodal decomposition is not taken into account. For references

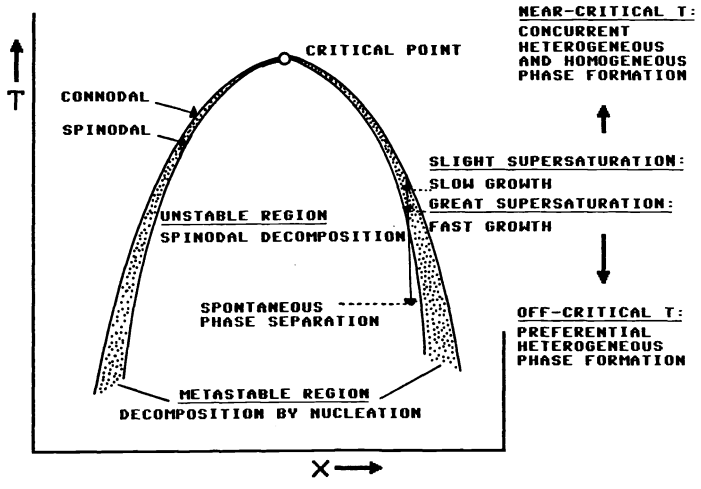

Fig. 2. Isobaric T(x) phase diagram of a binary system exhibiting gas-liquid critical phenomena and phase formation effects (see text)
(concerning own work and publications from the literature see refs. 28, 29, 32, 33, 35)

INVESTIGATIONS ON LIQUID-LIQUID SYSTEMS

Starting from this thermodynamic view of the phenomenon of liquid-liquid phase separation, we were confronted with the experimental observation of "instantaneous" decomposition when the coexistence curve in a system was reached (ref. 22). But just how fast is "instantaneous"? This question had also been raised in chemical reaction kinetics two decades earlier, and the answer had been the development of the so-called Relaxation Techniques (ref. 23). The cooperation with A. Jost, who had been a collaborator of M. Eigen at Göttingen before, gave us the opportunity to test this questioning with a temperature jump experiment.

In these investigations (ref. 24), a homogeneous solution of pyridine and water with a small amount of KCl added (in order to obtain sufficient electrical conductance) was heated from the discharge of a high-voltage capacitor by 2.4 to 5.4 K in a few microseconds; this is several orders of magnitude faster than in all former experiments. The onset of phase separation was monitored by the decrease of light transmission through the solution, and this revealed a continuous reduction of transmitted light intensity from 100% to 0% within milliseconds, starting with the moment of the temperature jump.

Light scattering experiments

As the loss of light transmittance is due to the onset of light scattering, the transmitted light gives a rough overall picture of the process only. Observation of a defined portion of the scattered light gives much more detailed information about the process, and U. Limbach (ref. 25) designed a temperature jump apparatus for the measurement of rectangularly scattered light (Fig. 3). For the interpretation of his results he adopted the Mie Theory (ref. 26) as up-to-date most comprehensive method for the evaluation of light scattering. From numerous experiments in the system 1-propanol + H_2O + KCl he found a diffusion controlled growth of droplets of the precipitating phase, but again there could not be found any distinct time-lag in the onset of phase decomposition.

Because the temperature jump technique had some disadvantages for the investigation of phase separation (the addition of salts for sufficient electrical conductance influences the miscibility gap, repetitive electrical discharges alter the solutions), J. Wenzel adopted the pressure jump technique (ref. 27) for his experiments. His optical autoclave (Fig. 4a) also had the third window for the observation of rectangularly scattered light: The incident light beam enters the cell through a sapphire window of 10 mm thickness. Two windows with the same dimensions permit observation of transmitted and scattered light. The schematic Fig. 4b elucidates the principle of the experimental set-up. The volume between an elastic membrane (EM) and a rupture diaphragm (RD) is pressurized until the strained diaphragm material bursts and so gives rise to a sudden pressure drop in the entire system. A magnetic stirring device for re-homogenisation of a heterogeneous mixture works below the plane of optical observation. With a high-speed pressure transducer (Kistler) the pressure - time profile during the pressure jump was detected. The temperature of the sample could be maintained constant by circulating thermostated water through vertical boreholes in the autoclave (not shown in Fig. 4a). A fast-change positio-

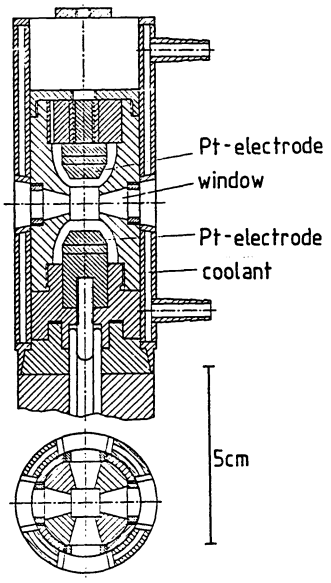

Fig. 3. Temperature-jump cell

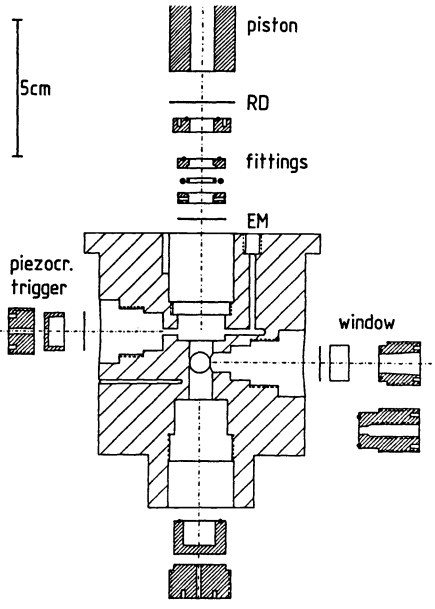

Fig. 4a. Pressure-jump cell

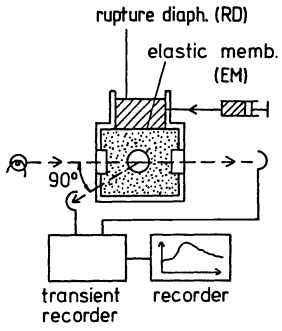

Fig. 4b. Principle of pressure-jump technique

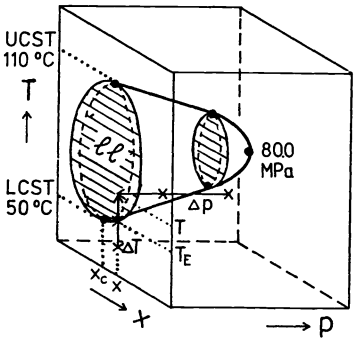

Fig. 5. Miscibility gap of 2-butoxyethanol + water in the p-T-x space (schematic)

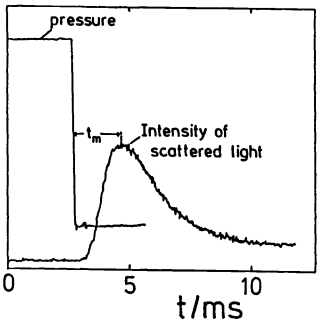

Fig. 6. Evaluation of characteristic time t_m for liquid-liquid systems

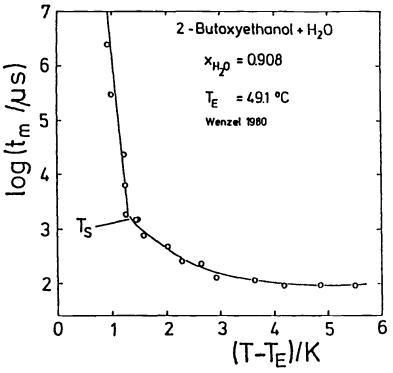

Fig. 7. Dependence of t_m on quench depth

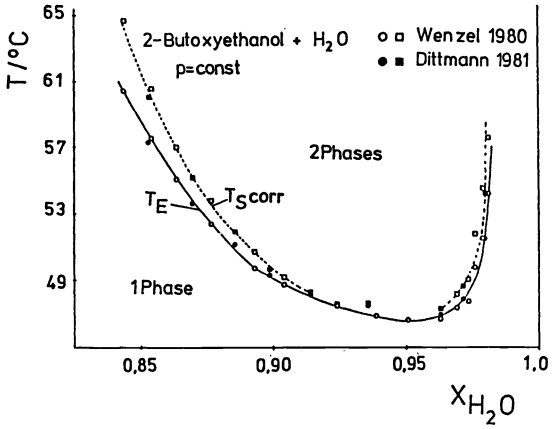

Fig. 8. T(x) phase diagram of a LCST system for p = const = 0.1 MPa (T_S= "branch-off" temperatures)

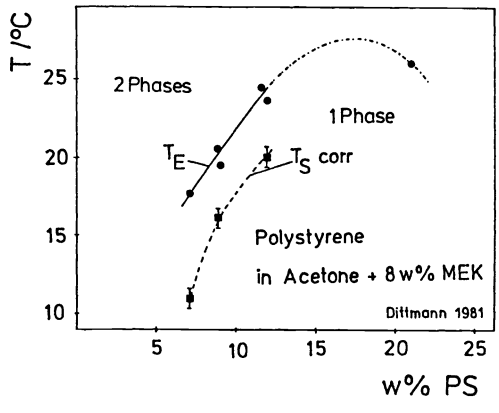

Fig. 9. T(x) phase diagram of a UCST system for p = const = 0.1 MPa (T_S= "branch-off" temperatures)

ning mechanism for an adequate strip of the rupture diaphragm material allowed high repetition frequencies for the experiments (refs 28, 29).

The apparatus was designed for the investigation of systems showing increasing mutual miscibility with rising pressures. The temperature of the experiment was adjusted under pressure and at homogeneous conditions; the subsequent pressure jump to ambient pressure displaced the system to heterogeneous conditions. In this way, the pressure jump at the desired temperature has the same effect as a temperature jump at ambient pressure to this temperature (Fig. 5).

In a series of experiments with the system 2-butoxyethanol + H_2O J. Wenzel found that the development of the first maximum of scattered light intensity as a function of time (Fig. 6) was faster with deeper penetration into the miscibility gap (i.e. temperature difference between the connodal and the experimentally adjusted temperature for a given composition and corrected for adiabatic effects; ref. 28). The period t_m from the initialization of phase separation to the first maximum varied between 10^1 and 10^{-4} seconds where the evaluation of this maximum indicates a defined state in the progress of droplet growth according to the theory of G. Mie (for details see refs 25,26). The variation of t_m is large in the vicinity of the coexistence curve (covering about four orders of magnitude!) and becomes much smaller for deeper quenches (Fig. 7). The plot time t_m for the development of the first Mie maximum vs. quench depth into the miscibility gap exhibits a sharp change for these two kinds of kinetic behaviour. Therefore the quench depth for this change is identified with a locus that is near to the so-called spinodal mentioned in the Introduction. The plot of the coexistence curve together with these "spinodal" temperatures (Fig. 8) shows the expected behaviour. These results have been confirmed by measurements with the systems nitrobenzene + 2-methylbutane and polystyrene ($\bar{M}_w = 20{,}400$ g.mol^{-1}; $\bar{M}_w/\bar{M}_n = 1.01$) + acetone + 8 w% 2-butanone (Fig. 9) which exhibit upper critical solution temperatures (UCST) and also increasing mutual miscibility with increasing pressure.

In this context G. Bresonik continued experiments of U. Limbach who had tried to monitor the temperature change during the temperature jump by the addition of a proton-coupled dye (system: triethylamine + H_2O; dye: trans-pyridine-2-azodimethylaniline. In these experiments the regular exponential time dependence of transmitted light intensity (which is a measure of temperature) due to the discharge characteristics of the high-voltage capacitor through the solution exhibits a sudden discontinuity for larger temperature jumps (ref. 28). Another series of temperature jump experiments with the same system (but without addition of dye) showed that the "spinodal" temperatures found with Wenzel's light scattering method were consistent with the results of Bresonik's dye method. Without going into details, this is supposed to be a support for the above-mentioned spinodal hypothesis since we are considering two completely different indicators of phase decomposition.

From these experiments, a distinct time-lag between penetrating a two-phase region and the onset of phase decomposition could not be found in contrast to the well-known superheating and undercooling effects e.g. for gas-liquid equilibria. However, in liquid-liquid systems the interfacial tension between bulk and nascent phase is very small, and due to this fact there is no important energy barrier for the formation of a supercritical nucleus. In this way the results of our experiments gave no hint on longer periods of metastability in liquid-liquid systems within the time resolution of the equipment (ref. 29), but the switch-over in kinetic behaviour is an indicator for approaching the stability limit or so-called spinodal. The same effect had been found earlier with the PICS-method by other authors (ref. 30) in polymer solutions where the high molecular mass leads to a much slower droplet growth so that a conventional cooling pulse of the order of seconds was applicable in these investigations.

Observation of ageing effects

Theoretical calculations of scattered light intensities according to the theory of G. Mie were in good agreement with experimental curves. Therefore the assumption of a monodisperse distribution function of droplet radii should approximately hold for the time until the first Mie maximum has occurred (ref. 25). It had to be expected, however, that with further increasing time after the pressure quench amongst other effects (e.g. multiple scattering) an increasing importance of polydispersity has to be taken into account. For this period it was desirable to get informations on the late state growth of the precipitate.

In order to make use of the advantages of this technique a pressure jump cell

for direct microscopical observations was constructed and improved (ref. 31). The cylindrical pressure vessel (Fig. 10) consists of stainless steel. The two windows are made from sapphire cylinders with a diameter of 25 mm and thicknesses of 5 and 10 mm respectively, the observation diameter being 22 mm. The maximum working pressure allowed is about 20 MPa. Pressure connection to the sample compartment is accomplished through a 5 mm hole with a countersink cone boring of 10 mm diameter that embraces an elastic pressure transducing membrane (usually 'Kalrez'; DuPont). The membrane separates the sample liquid from the pressurizing medium (usually water). A 'swagelock' T-junction is connected to the pressurizing inlet. It contains the rupture diaphragm; depending on the thickness of this aluminium disk, the pressure jump amplitude may be varied up to 15 MPa. The temperature of the cell can be maintained constant by circulating a thermostating liquid through two channels in the upper and lower front surface that are connected by 24 axial borings. A temperature sensor can be placed in a 1.5 mm diameter hole very close to the sample compartment between the windows. The autoclave is mounted in a commercial transmission microscope and illuminated from below. Sample thickness might be varied between 2 and 0.4 mm by the use of different distance rings in the cell assembly. The microscope can be focussed within the entire height of the sample by the use of a special objective lens allowing large working distances. A 16 mm film camera or alternatively a video camera is mounted on the microscope for the registration of the pressure induced process. The whole arrangement is placed on a shock and vibration absorbing table. The registration system is equipped with an event marker triggered electronically. By a microcomputer temperature, pressure, and plane of focus are controlled or monitored respectively. A "home-made" low-cost digitizing system permits storage and processing of optical information with a resolution of 255 × 255 pixels each containing information about one of 16 grey levels. Fig. 11 gives a schematical representation of the experimental setup. Positive pressure pulses might be triggered and performed within 100 ms by an electromagnetically worked valve.

An example for the ageing process in the above-described system 2-butoxyethanol + H_2O is given in Fig. 12a-d. In Fig. 12a the system has just passed the connodal line by a negative pressure jump of 14.3 MPa and 150 μs duration. The first visible droplets occur within about 100 ms. They are of approximately equal size of 8 to 10 μm that is the limit of the resolution of the microscope. After 42 s (see Fig. 12b) the droplets of the precipitate show a nearly uniform size of about 18 μm. 44 s later some droplets become fixed to the upper cell window. According to gravitation the droplets of the lighter 2-butoxyethanol-rich phase undergo growth by coalescence of macroscopic droplets at the upper window (Fig. 12c). More than 4 min after initializing phase separation (Fig. 12d) it is evident that diffusion controlled growth being observable in our

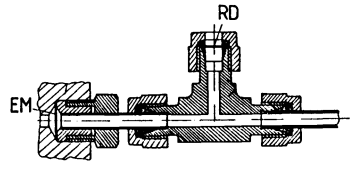

Fig. 10. Microscope cell (left) with rupture diaphragm support (right)

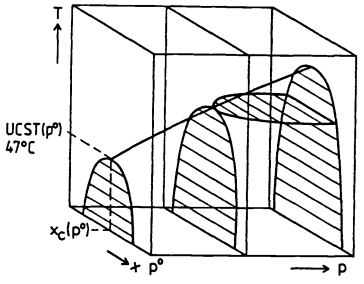

Fig. 13. Liquid-liquid phase equilibria of cyclohexane + methanol in the p-T-x space (schematic)

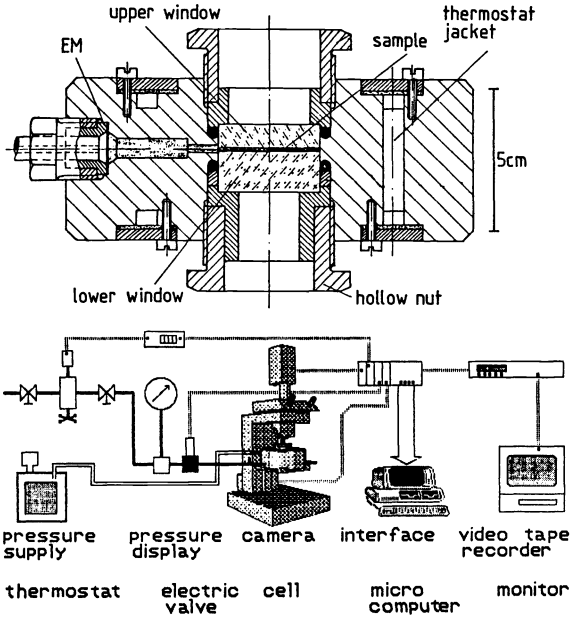

Fig. 11. Experimental set-up for microscope observations

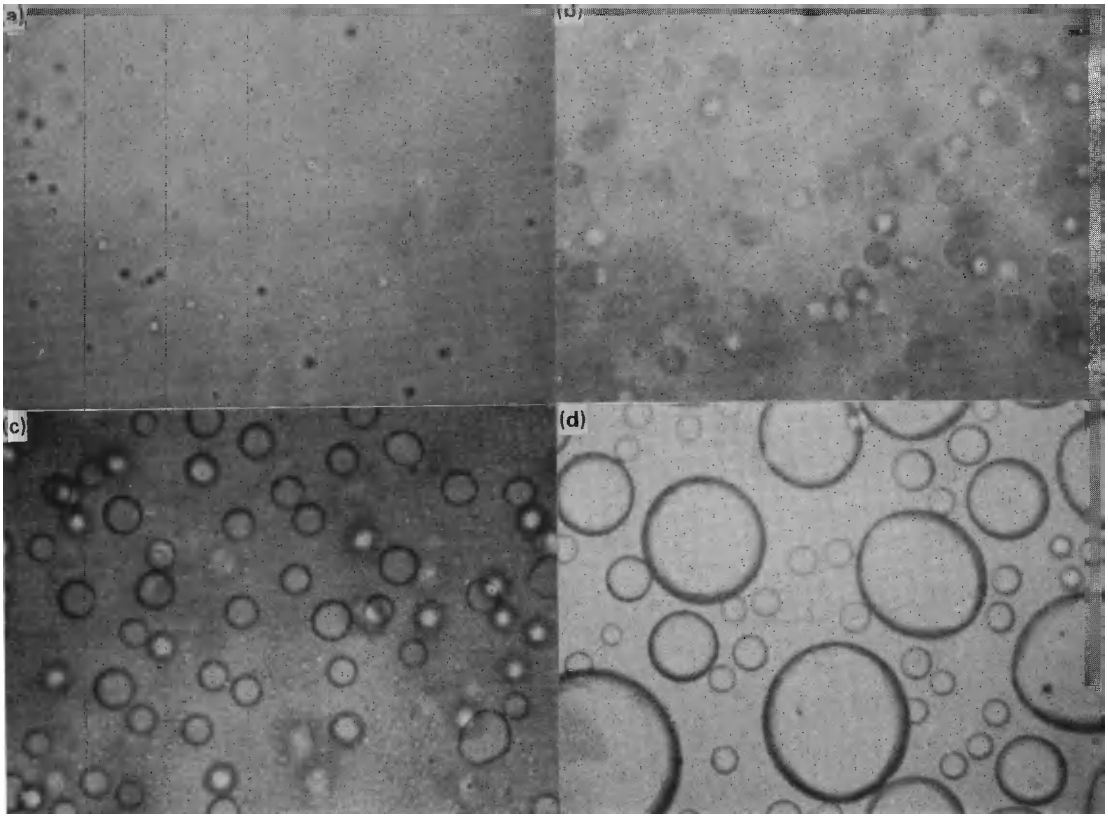

Fig. 12. Ageing by coalescence under gravity in the system 2-butoxyethanol + H_2O (12 w% 2-butoxyethanol; 53.7 °C; for details see text)
Time after pressure jump: (a) about 1 s; (b) 42 s; (c) 86 s; (d) about 4 min

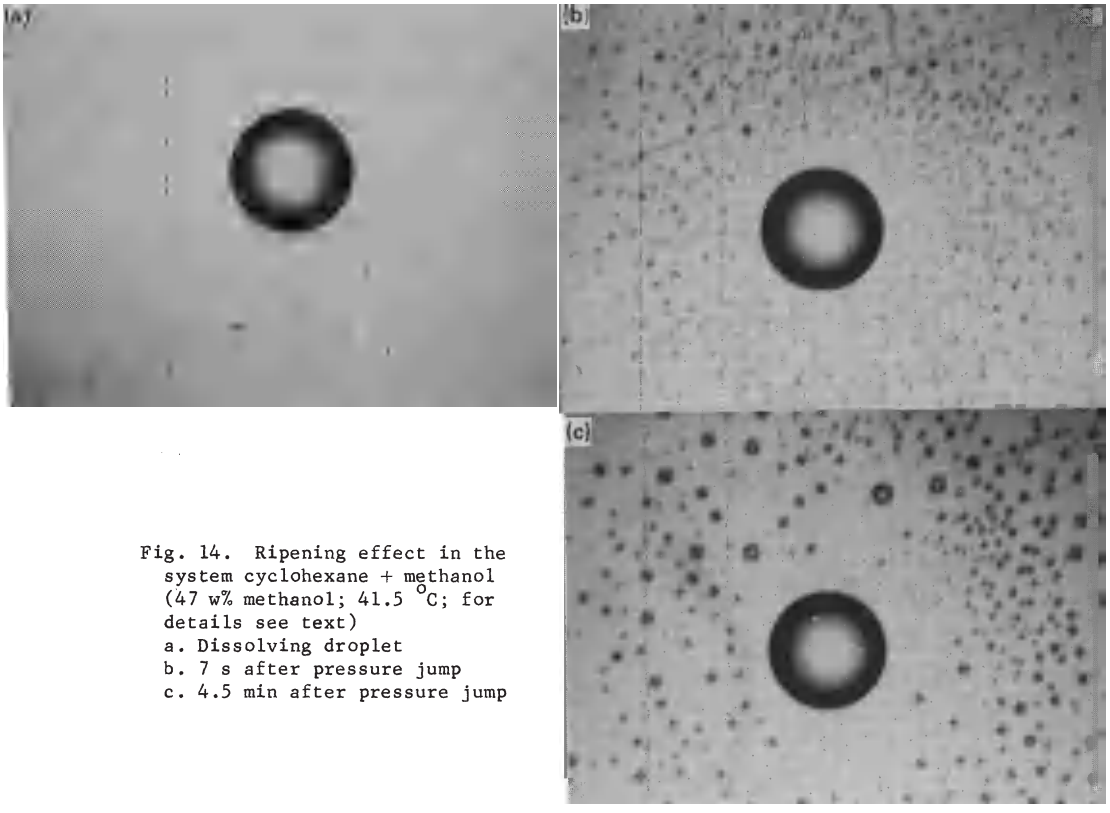

Fig. 14. Ripening effect in the system cyclohexane + methanol (47 w% methanol; 41.5 °C; for details see text)
a. Dissolving droplet
b. 7 s after pressure jump
c. 4.5 min after pressure jump

facing page 84

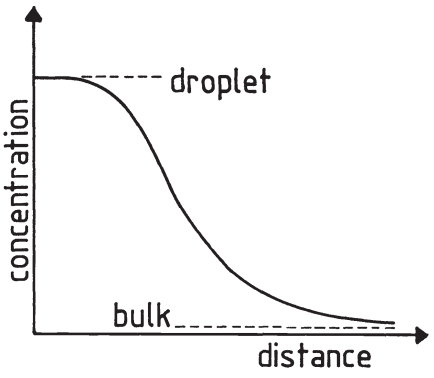

Fig. 15. Illustration of cyclohexane supersaturation progress along a radial path from droplet to bulk phase (for initial experimental conditions see Fig. 14)

(a) (b)

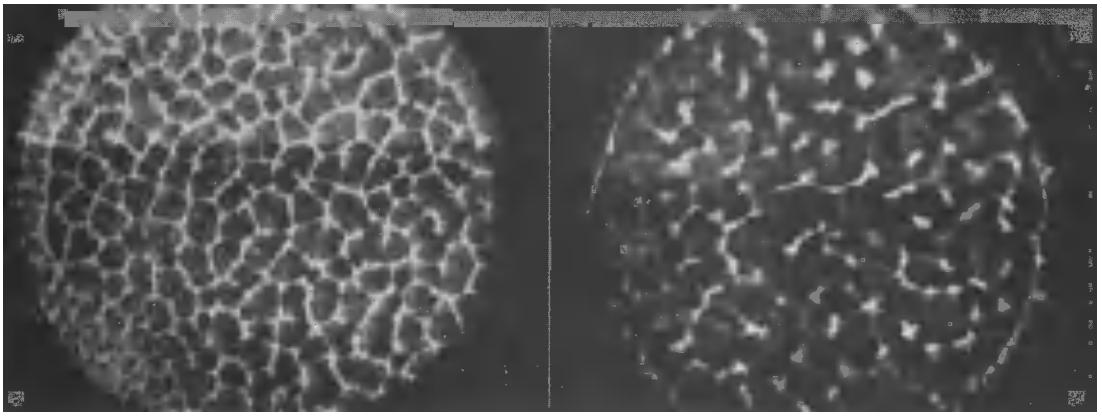

Fig. 16. Dissipative structure in the system cyclohexane + methanol (see text)
a. Layer depth 0.8 mm b. Layer depth 2.0 mm

(a) (b)

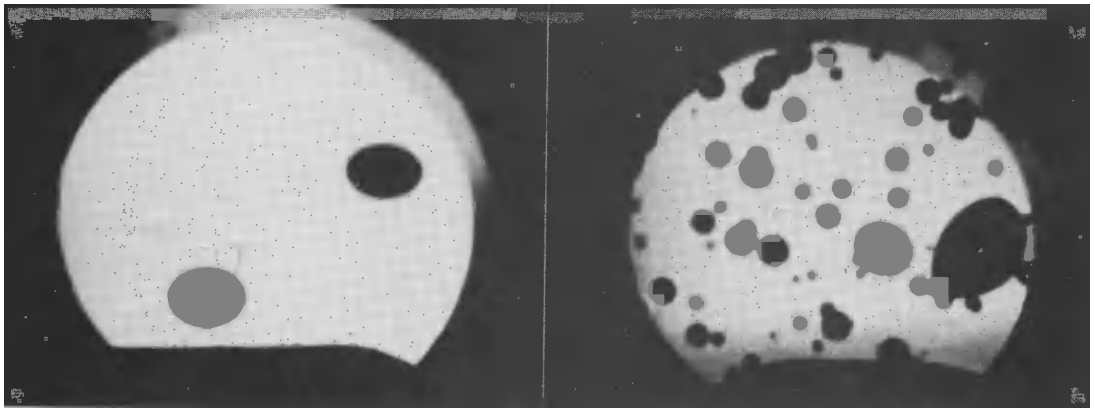

Fig. 17. Pressure induced formation of nitrogen bubbles in liquid benzene at 0.1 MPa and room temperature after saturation at 2.5 MPa
a. Without stirring b. During stirring

time scale already stopped within about 40 s after the pressure jump because smaller droplets dominating in Fig. 12b are still amongst the population on the upper window, whereas the free sample space does practically not contain anymore droplets. These small droplets didn't undergo coalescence and therefore maintained their size.

Similar experiments at different initial supersaturations and compositions of the mixture demonstrated that the precipitate we could observe is monodisperse even at long times after the pressure quench and that coarsening by coalescence in the gravitational field leads to a visible polydisperse distribution of droplet radii. Thus an important assumption for the validity of light scattering experiments in the preceding chapter should be fulfilled. Unfortunately the size-gap between diameters of 300 nm (light scattering) and 5000 nm (microscope observations) could not be covered by our investigations. From our observations we conclude that a broadening of the size distribution in liquid-liquid systems by coagulation kinetics (concerning Smoluchowski's theory) and diffusion controlled coarsening (Ostwald ripening) is of minor importance.

Investigations on isopycnic systems

In order to eliminate droplet motion in the gravitational field a system where the coexisting phases have nearly equal densities after separation (so-called isopycnic system) was chosen. A schematic phase diagram of the cyclohexane + methanol system is shown in Fig. 13. Here the density differences of the pure substances amount to 0.01 $g \cdot cm^{-3}$ only instead of 0.1 $g \cdot cm^{-3}$ in the 2-butoxyethanol + H_2O system. Exhibiting an upper critical solution temperature (UCST) of about 47°C it matches the conditions for an investigation in our experimental setup. The option for positive pressure jumps, however, had to be used because here the mutual miscibility decreases with increasing pressure. Although the motion of droplets in this system was much slower, an undisturbed observation of Ostwald ripening was not yet possible.

With the intention to get an idea of this process the system was shorthand forced to undergo diffusion controlled coarsening in the following manner. Fig. 14a shows a droplet of about 70 µm diameter consisting of the cyclohexane-rich phase fixed at the upper cell window. The droplet is dissolving because the system is actually under homogeneous conditions (0.1 MPa). A schematic representation of the cyclohexane concentration in the vicinity of the droplet is given in Fig. 15. After a positive pressure jump to heterogeneous conditions (3 MPa) the cyclohexane-rich phase separates in the diffusion range around the big droplet that is now again in a stable (nondissolving) state. Fig. 14b represents the situation described above seven seconds after the pressure jump. During a long time period (4.5 min) with the system resting under these conditions a coarsening can be observed (Fig. 14c): Small droplets in the vicinity of the big droplet have completely vanished whereas the droplets in some distance remain and even increase in size. A plain description of the process might be deduced from diffusion controlled growth of a sphere and the well-known Gibbs-Thompson relationship

$$\frac{dr}{dt} = \dot{r} = \frac{D \cdot c_\infty}{V_m \cdot r} \cdot \left(\Delta c - \frac{L}{r}\right)$$

with $L = \frac{2 \cdot \sigma \cdot V_m}{R \cdot T}$ being the so-called capillary length (where σ = interfacial tension)

and $\Delta c \equiv \frac{c(t) - c_\infty}{c_\infty}$ a dimensionless time dependent supersaturation.

It results from the equation given that $\dot{r}$ becomes negative if $r < L/\Delta c$. As a consequence the particle dissolves if Δc becomes small at the end of precipitation. Thus a small particle has to dissolve in favour of a big one with $r > L/\Delta c$.

Our experiment shows Ostwald ripening within the experimental observation time only in the immediate neighbourhood of a big "artificially" made particle. In comparison to the time scale for coalescence ageing it is evident that this process could not be observed in a "normal" liquid-liquid demixing experiment (for details see ref. 34).

Dissipative structures induced by phase separation

Further investigations of the near isopycnic system cyclohexane + methanol revealed an amazing effect (ref. 35). Fig. 16a and 16b show the top-view of the circular upper window of the microscope cell (22 mm diameter). The cell contains a mixture of x(methanol) = 0.75 at 39°C after a positive pressure pulse

of 5 MPa that led to phase separation. The dark regions visible consist of vertically gyrating droplets due to a convective motion, whereas the separating light channels contain no precipitate. These structures are induced by the process of phase separation itself and not from a temperature gradient alone since a gradient of about 0.5 K between the windows was already present before the pressure quench.

This dissipative structure is closely related to the Rayleigh-Bénard Instability (RBI) as confirmed by the influence of layer depth on structure dimensions (see ref. 35). The RBI is determined by the Rayleigh number

$$Ra \sim g \cdot \Delta T \cdot d^3$$

where d = layer depth, g = gravity, and ΔT = temperature difference.

In case that Ra exceeds a critical value Ra(crit) of about 1700 heat transport is accomplished by convective motion rather than by heat conduction. Near Ra(crit) convection leads to the exhibition of hexagonal structures (ref. 36). In systems with larger density differences e.g. 2-butoxyethanol + H_2O no structures develop, and any structure could neither be observed in a system that matches nearly ideal isopycnic conditions (e.g. cyclohexane + methanol with the addition of 1 mol% C_2Cl_4 where $\Delta\rho \approx 0.001$ g·cm^{-3}). These effects may become important in space experiments (e.g. for the preparation of alloys from heterogeneous melts) where small residual accelerations (e.g. of the order of 0.001 g) may influence mixtures having high density differences (e.g. of the order of 10^{1} g·cm^{-3}) between coexisting phases.

EXTENSION TO GAS-LIQUID SYSTEMS

Parallel to the liquid-liquid experiments with the observation of visible droplets J. Wenzel started investigations on gas-liquid systems as a contribution to the field of hyperbaric physiology where he employed a prototype of the pressure jump cell described above. For the experiments the cell was filled with the liquid under observation. The gas was directly contacted with the liquid surface and saturation was obtained by pressurizing (approx. 2.5 MPa) and magnetically stirring for approximately one hour. Then the diaphragm was ruptured by a sudden pressure increase, and the gas bubbles formed were registrated by high speed photography (ref. 33).

Observation of metastability effects

Soon it became evident that - unlike in liquid-liquid systems - here the phase separation proceeded via heterogeneous nucleation. Few and large aggregates of the gas phase moved upwards and could be photographed through the cell cross-section under observation (Fig. 17a). These aggregates were formed at the bottom of the pressure vessel at various discontinuities due to machining and when rising were ellipsoidically deformed under the combined influences of gravitational and frictional forces in the liquid bulk phase. On their gravity induced way upwards they collected excess gas in the supersaturated solution and therefore increased in size leaving behind typical schlieren patterns due to the concentration gradients formed. When the ascending of gas bubbles ceased the stirring device was switched on. The registrated picture shows that a large amount of gas remained in the system (Fig. 17b). This gas volume could have been formed in the previously mentioned manner remaining fixed at the bottom of the cell until stirring. On the other hand it could have been formed in the free solution by turbulences from stirring. The heterogeneous size distribution indicates that both influences became effective.

These preliminary results made evident that simultaneous observation of the whole liquid phase was indispensable, and J. Wenzel designed an all-glass pressure jump cell (Fig. 18) where the bubbles formed by heterogeneous nucleation could be detected and observed at the places of their origin. A series of experiments performed by J. Becker demonstrated that the main origin of growing bubbles were small gas enclosures that persisted at the rough surfaces during pressurizing whereas the existence or formation of fluid-fluid or fluid-solid interface was of minor importance. This is an important finding which confirms the current view in hyperbaric physiology with respect to the origin of gas bubbles in the decompression process (ref. 41).

Light scattering investigations on nascent gas bubbles

In these experiments gas-liquid mixtures differed considerably from the liquid-liquid systems that were investigated previously. For theoretical reasons it became desirable to relate the gas-liquid investigations to our liquid-liquid observations. The obvious difference between the two kinds of systems is the by far larger interfacial energy in the gas-liquid systems (refs.

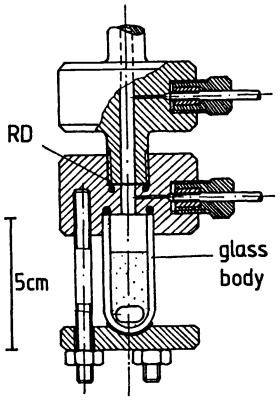

Fig. 18
All-glass cell

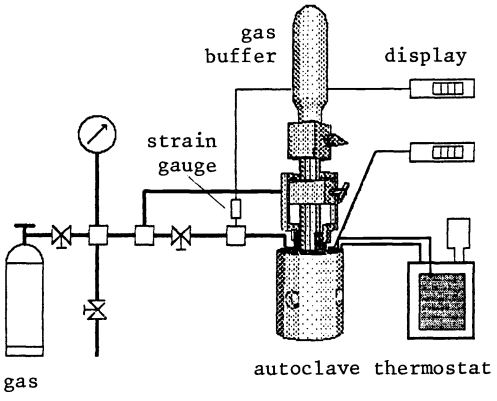

Fig. 19
Set-up for light scattering experiments on liquid-gas systems

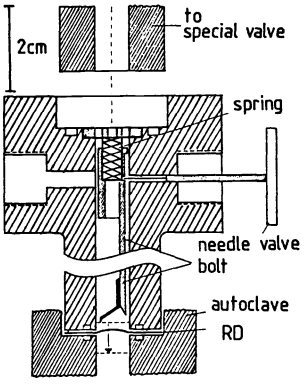

Fig. 20
Bolt mechanism for performing moderate p-jumps in lg systems

32, 33). In the vicinity of a critical point, however, the interfacial tension should decrease as usual and we tried to find a system where this could be accomplished within the temperature and pressure range of our experimental hardware.

The expected effect was first studied in the system CO_2 + decane, then in the more suitable system ethene + hexane. An increase in saturation pressure of only a few tenth of a MPa in the range of 5.0 MPa towards the critical pressure of 5.8 MPa at 20°C resulted in a dramatical change of the behaviour. Whereas the effects found under off-critical conditions were essentially the same as descibed above for gas-liquid systems, the phase decomposition in the vicinity of the critical point started within the first 10^{-1} s and resembled very much to that of liquid-liquid systems until the aggregates of the gaseous phase had increased in size to be able to leave the positions where they had been formed.

The experiments with direct visual observation were only of limited value and it became interesting to see whether the light scattering method from our liquid-liquid experiments could also be applied here. M. Dittmann and J. Wenzel employed the same apparatus as in their former liquid-liquid light scattering experiments and found a similar behaviour. This opened the way for U. Metz to conduct systematic investigations with an improved apparatus (ref. 37).

The more recent phase separation experiments on liquid-gas systems were carried out in an improved version of the pressure jump cell shown in Fig. 4a. The new cell consists of two parts: the lower portion that contains the liquid sample saturated with gas and the upper portion for generating the pressure difference. Both parts are separated by a rupture diaphragm of aluminium. Fig. 19 gives a schematic view of the setup used for these light scattering studies. In the experiments the cell (volume about 5 cm^3) is filled with the liquid sample from the top and saturation with the gaseous component is accomplished by compression with the gas from a reservoir.

A special feature of the improved pressure jump apparatus is a mechanism that allows the rupture of the membrane while having a definite pressure difference between sample cell and gas compartment (Fig. 20). Here a bolt with an appropriate cutting edge and driven by a spiral spring is released from outside the autoclave by a modified needle valve mechanism and destroys the membrane. The pressure inside the sample cell is registrated by a high-precision strain gauge (Burster) whereas the pressure in the gas compartment is measured by a manometer.

An important aspect for generating definite differential pressure jumps in gas-liquid systems is to optimize the relative dimensions of the sample cell and the gas chamber respectively. On this account an additional pressure vessel (volume about 500 cm^3) was integrated in the pressure design in such a way that it was aligned with the pressure jump apparatus. Because of the necessity

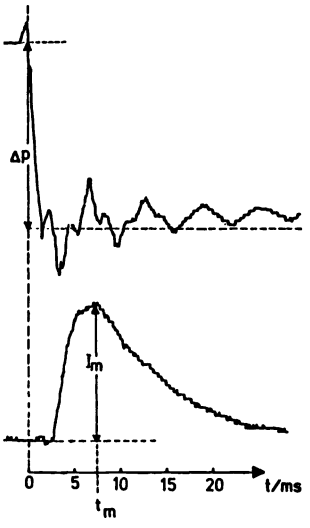

Fig. 21 Experimental curves from p-jump investigations on a liquid-gas system (analogon to Fig. 6)

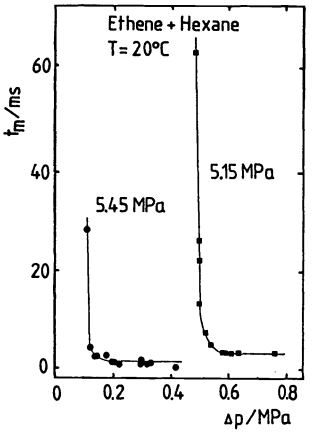

Fig. 22 Dependence of t_m on quench depth (analogon to Fig. 7)

of changing the membrane before each experiment and therefore of demounting the whole pressure apparatus it was advantageous to separate the additional gas vessel from the main setup by a valve. The valve was only opened when carrying out pressure jump experiments and closed when refilling the cell so that the gas reservoir could be used for the next run without loss of gas. A special valve with a flow diameter of 10 mm was chosen in order to hinder the pressure jump as slightly as possible. With this apparatus it was possible to carry out positive as well as negative pressure jumps. The quench depth could be varied from 0.05 to 1 MPa by using membranes with a thickness of 0.06 mm (normal bursting pressure approx. 1.4 MPa). The duration of the pressure jumps could be limited to 1 - 5 milliseconds depending on the quench depth, on the initial pressure and also on the properties of the medium under test.

The intensity of light scattered by the liquid sample is detected by a photomultiplier at 90° with respect to the incident beam of a 5 mW He-Ne laser. The intensity vs. time curve is stored in a 5 MHz transient recorder which is triggered by the signal of the pressure transducer. The pressure vs. time profile is also recorded by a second transient recorder, the sampling being made synchronously at the same time base. The stored signals can be monitored using an oscilloscope and also be recorded on an X-Y plotter. The upper curve in Fig. 21 shows a typical pressure jump profile obtained from measurements with a sample of ethene + hexane. The pressure relaxation is characterized by a strongly damped oscillation when approaching the adjusted difference pressure. In the lower curve a Mie maximum is exhibited.

Similar to the experiments of J. Wenzel the time dependent appearance of the first Mie maximum in scattered light intensity during the early stage of phase separation was measured. This time which is correlated to a definite radius of the particles of the precipitating phase is plotted vs. the quench depth in Fig. 22 for two different initial saturation pressures at equilibrium. The curves are characterized by two different branches: The nearly horizontal branch at deeper quenches only exhibits a negligible dependence on quench depth whereas the nearly vertical branch at lower quenches into the miscibility gap is characterized by a strong dependence on supersaturation.

Recent developments

Since in gas-liquid systems the interfacial tension varies rather strongly even in the off-critical region of the phase diagram, they will be ideal systems to study the different mechanisms of homogeneous and heterogeneous nucleation. Further developments aim at a more quantitative approach to these effects. Recent activities of U. Metz resulted in the construction of an improved measuring device (Fig. 23) where scattered light can be observed at two variable angles with respect to the plane of incident light (ref. 39). The

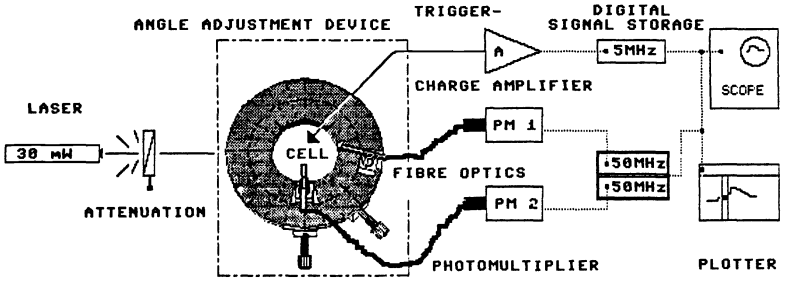

Fig. 23 Optoelectronic set-up for light scattering measurements at variable angles on fluid systems under pressure (cell based on the all-glass cell given in Fig. 18)

setup, principally based on the all-glass pressure cell, covers a pressure range of 1 to 8 MPa and a temperature range of 298 to 333 K. Concerning the thermodynamic properties of the gas-liquid systems that are considered in our investigations, it is important that the critical curve of the mixture runs through these ranges. Therefore the critical point of the gaseous component should approximately fit to the lower limits of our experimental pressure and temperature ranges. There are only few substances as gaseous components (e.g. CHF_3, C_2H_6, SF_6, CO_2) that are compatible with these conditions. However, substances exhibiting critical temperatures far above those of these gases respectively, may serve as liquid components in our experiments (e.g. hexane, cyclohexane, benzene).

A pressure jump autoclave for investigations in the high-pressure range (0 to 300 MPa; up to 200°C) was developed by J. Quednau. The cell, presently under test, is capable of performing differential pressure jumps of max. 15 MPa (ref. 40).

Financial support of the Bundesminister für Forschung und Technologie (BMFT) through the Deutsche Forschungs- und Versuchsanstalt für Luft- und Raumfahrt e.V. (DFVLR) is gratefully acknowledged.

REFERENCES

1. J. Thoen, Leuven, invited lecture presented at the 9th IUPAC Conference on Chemical Thermodynamics, Lisbon, Portugal, 14 - 18 July 1986, Paper 7.19. (High-Resolution Calorimetry Near Phase Transitions of Liquid Crystals).
2. O. Yamamuro, M. Oguni, T. Matsuo, and H. Suga, Osaka, as ref. 1, Paper 7.4. (A High-Pressure Adiabatic Calorimeter with Gaseous Medium).
3. A. Heintz and R.N. Lichtenthaler, Heidelberg, as ref. 1, Paper 7.15. (Excess Enthalpies of Fluid Mixtures at High Pressure. Experimental Techniques Available and Future Trends).
4. R. Castro-Gomez, J.C. Holste, K.R. Hall, and K.N. Marsh, Texas A&M, as ref. 1, Paper 7.12. (A Thermoelectric Total Enthalpy Flow Calorimeter).
5. C. Alba, Paris, as ref. 1, Paper 7.23. (An Innovative Isothermal Calorimeter and Piezothermal Method Advances Applied to Thermodynamics of Fluid State under Pressure).
6. F. Pavese, Turin, as ref. 1, Paper 7.6. (Adiabatic Calorimetry with Sealed Samples: A Modern Technique for Studies of Thermodynamic Properties of Pure Gases in the Liquid-Solid State).
7. Å. Fransson and G. Bäckström, Umea, as ref. 1, Paper 7.21. (DSC Measurements of Isothermal Enthalpy Relaxation).
8. F. Kohler and K. Holzapfel, Bochum, as ref. 1, Paper 7.1. (Routine Density Determination over an Extended Temperature Range and up to 1000 bar).
9. J.C. Holste, G.A. Iglesias-Silva, W.R. Lau, K.R. Hall, P.T. Eubank, and K.N. Marsh, Texas A&M, as ref. 1, Paper 7.13. (A High Pressure Pyknometer for Fluid Density Measurements).
10. H. Häusler, K. Kerl, and S. Schwarzer, Braunschweig, as ref. 1, Paper 7.7. (Determination of Second and Third Virial Coefficients of Some Gases and Gas Mixtures by Optical Interferometry).
11. G. Tardajos, M. Diaz Peña, and E. Aicart, Madrid, as ref. 1, Paper 7.8. (A Pulse-Echo-Overlap Technique to Measure the Speed of Sound in Liquids).

12. G.J. Esper, Bochum, as ref. 1, Paper 7.2. (Semiautomated Measurements of Second Acoustic Virial Coefficient).
13. M.B. Ewing, A.R.H. Goodwin, M.L. McGlashan, and J.P.M. Trusler, London, as ref. 1, Paper 7.9. (Measurement of the Speed of Sound in Gases at High Pressures Using Spherical Resonators).
14. Y. Takahashi, Tokyo, invited lecture, as ref. 1, Paper 7.20. (Laser-Flash Calorimetry - Experimental Technique and Some Applications).
15. M.G. Frohberg, Berlin, as ref. 1, Paper 7.18. (Enthalpy Measurements on Refractory Metals and Alloys by Levitation Calorimetry).
16. R.L. Berger, Bethesda, and N. Davids, University Park, as ref. 1, Paper 7.14. (Thermal Instrument Response Deconvolution by Finite Element Simulation).
17. A.L. Ruoff, Cornell, invited lecture, as ref. 1, Paper 7.5. (Science at One Megabar and Above).
18. J.A. Schouten, Amsterdam, invited lecture, as ref. 1, Paper 7.10. (Determination of Phase Equilibria in Fluid Mixtures in a Diamond Anvil Cell up to 100 kbar).
19. J. Christensen, D.R. Cordray, and R.M. Izatt, Provo, as ref. 1, Paper 7.16. (The Use of Flow Calorimetry to Determine Thermal Effects, Regions of Immiscibility and Phase Composition at High Temperatures and Pressures).
20. W.J. Rogers, J.C. Holste, K.R. Hall, P.T. Eubank, and K.N. Marsh, Texas A&M, as ref. 1, Paper 7.11. (A Microwave Phase Boundary Apparatus).
21. G.M. Schneider, M. Dittmann, U. Metz, and J. Wenzel, Bochum, invited lecture, as ref. 1, Paper 7.3. (Kinetics of Phase Separation in Fluid Mixtures by Relaxation Methods: Pressure-Jump Experiments and Selected Results).
22. G.M. Schneider, Ber. Bunsenges. Phys. Chem. 70, 497 - 520 (1966).
23. M. Eigen and L. De Maeyer, in: Techniques of Chemistry, 3rd Edition. (A. Weissberger, ed.), Vol.VI, Part II, Chap.3, Wiley-Interscience, 1974.
24. A. Jost and G.M. Schneider, J. Phys. Chem. 79, 858 (1975).
25. U. Limbach, A. Jost, and G.M. Schneider, J. Phys. Chem. 80, 1952 - 1953 (1976).
26. G. Mie, Ann. Phys. (Leipzig) 25, 377 - 445 (1908).
27. W. Knoche, in 23., Chap. 5.
28. J. Wenzel, U. Limbach, G. Bresonik, and G.M. Schneider, J. Phys. Chem. 84, 1991 - 1995 (1980).
29. J. Wenzel, Doctoral Thesis, University of Bochum, 1980.
30. K.W. Derham, J. Goldsbrough, and M. Gordon, Pure & Appl. Chem. 38, 97 - 116 (1974).
31. J. Wenzel and G.M. Schneider, Rev. Sci. Instrum. 52, 1889 - 1890 (1981).
32. G.M. Schneider, M. Dittmann, and J. Wenzel, in: Spacelab-Nutzung, Status-Seminar 1980 des Bundesministeriums für Forschung und Technologie, Deutsche Gesellschaft für Luft- und Raumfahrt e.V., DGLR-Report 80-02, 1980.
33. G.M. Schneider, M. Dittmann, and J. Wenzel, as 32., Status-Seminar 1982, DGLR-Report 82-02, 1982.
34. M. Dittmann, Doctoral Thesis, University of Bochum, in preparation.
35. M. Dittmann and G.M. Schneider, Z. Naturforsch. 41a, 678 - 680 (1986).
36. S. Chandrasekhar, Hydrodynamic and Hydromagnetic Stability, Oxford University Press, London, 1961.
37. U. Metz, Diploma Thesis, University of Bochum, 1985.
38. J.S. Rowlinson and F.L. Swinton, Liquids and Liquid Mixtures, 3rd edition, Butterworths, 1982.
39. U. Metz, Doctoral Thesis, University of Bochum, in preparation.
40. J. Quednau, Doctoral Thesis, University of Bochum, in preparation.
41. P.B. Bennett and D.H. Elliott (eds), The Physiology and Medicine of Diving, 2nd edition, Baillière, Tindall, London, 1975.